JOURNAL OF SPACECRAFT AND ROCKETS
Vol. 44, No. 3, May–June 2007

# Geometrically Nonlinear Shell Analysis of Wrinkled Thin-Film Membranes with Stress Concentrations

Alexander Tessler* and David W. Sleight†
*NASA Langley Research Center, Hampton, Virginia 23681-2199*

DOI: 10.2514/1.22913

**Geometrically nonlinear shell finite element analysis has recently been applied to solar sail membrane problems to model the out-of-plane deformations due to structural wrinkling. Whereas certain problems lend themselves to achieving converged nonlinear solutions that compare favorably with experimental observations, solutions to tensioned membranes exhibiting high stress concentrations were difficult to obtain, even with the best nonlinear finite element codes and advanced shell-element technology. In this paper, two numerical studies are presented that pave the way to improving the modeling of this class of nonlinear problems. The studies address the issues of mesh refinement and stress-concentration alleviation and the effects of these modeling strategies on the ability to attain converged nonlinear deformations due to wrinkling. The numerical studies demonstrate that excessive mesh refinement in the regions of stress concentration may be disadvantageous to achieving wrinkled equilibrium states, causing the nonlinear solution to be biased toward the membrane response and totally discarding the very low-energy bending response that is necessary to cause wrinkling-deformation patterns.**

## Introduction

SOLAR sails are large thin-polymer film structures that use solar light for their propulsion. Because of their large size and operational use in a weightless space environment, full-scale solar sails spanning several hundred meters in length are particularly difficult to test in a laboratory, thus necessitating the need for validated computational models and methods for the design and analysis of future solar sail missions.

From the solid mechanics viewpoint, a thin-film solar sail is a membrane structure having a thickness that is several orders of magnitude smaller than its lateral dimensions. This structural characteristic implies that the bending stiffness is negligibly small compared with the membrane stiffness, and predominantly tensile membrane stresses develop due to applied tensile loading. There also exist, however, rather low compressive stresses that tend to wrinkle the material, producing geometrically large out-of-plane displacements. Because structural wrinkles in solar sails may detrimentally affect such principal parameters as stability, maneuverability, and reflectivity, an increased interest in research activities for structural wrinkling of thin membranes has been generated in recent years [1–8].

To enable computational modeling of wrinkling deformations, both membrane and bending flexibilities must be considered in the analytical model based on geometrically nonlinear kinematics with large displacements and rotations. Departing from classical tension-field theory [9], several recent computational studies have employed geometrically nonlinear shell finite element models [3–8]. Although some success was achieved, particularly when modeling wrinkled equilibrium states in relatively simple problems, the problems exhibiting high stress concentrations due to nonlinear geometrical effects were exceptionally difficult to solve, even with the best nonlinear finite element codes and advanced shell-element technology. There is still no consensus on how to consistently produce high-fidelity reliable solutions for this class of problems, as evidenced by the various approaches and their rather limited success and acceptability [3–8].

In a recent computational study, Tessler et. al. [3] employed a geometrically nonlinear, static shell analysis using the ABAQUS finite element code [10]. They demonstrated that for perfectly flat membranes, the onset of wrinkling deformations can be facilitated using small, pseudorandom, out-of-plane geometric imperfections imposed at the nodes. The approach of using pseudorandom imperfections is computationally unbiased, simple, and efficient, and proved to be effective, even for very low imperfection amplitudes and a wide range of spatial distributions. Additionally, the authors have proposed how to model the corner regions subjected to concentrated loads. To alleviate the deleterious effect of high stress concentration, they proposed to truncate the corner regions and to replace the concentrated loads with the statically equivalent distributed loads. This modeling strategy provides a simple means of 1) removing the severe stress concentration resulting from concentrated forces applied at corner nodes and 2) improving the corner region mesh quality and, hence, element performance. This modeling approach enabled physically realistic predictions of the deformations of a flat square membrane loaded in tension by corner loads.

In this paper, several key modeling features are explored that affect, to a significant degree, the formation of structural wrinkles in thin-membranes possessing stress concentrations. The focus problem is a flat, square, thin membrane loaded in tension at its four corners. Two finite element studies are undertaken to investigate key computational parameters to gain further insight into the proper modeling of wrinkling-deformation states in thin-film membranes with stress concentrations. The first study focuses on the mesh refinement strategy near the high stress-concentration regions, in which a tensile traction load is prescribed along a truncated corner of a membrane. The second study deals with the same membrane having various sizes of corner truncation.

In what follows, a thin-membrane test article and the corresponding finite element models are first described. Then the numerical results of two parametric studies are presented. These studies explore the improved modeling strategies in the regions of stress concentration that permit the formation of structural wrinkles in thin membranes.

Presented as Paper 1739 at the 45th AIAA/ASME/ASCE/AHS/ASC Structures, Structural Dynamics, and Materials Conference, Palm Springs, CA, 19–22 April 2006; received 1 February 2004; revision received 1 November 2006; accepted for publication 28 November 2006. 

*Aerospace Engineer, Structural Mechanics and Concepts Branch, Mail Stop 190, Research and Technology Directorate.

†Aerospace Engineer, Durability, Damage Tolerance, and Reliability Branch, Mail Stop 188E, Research and Technology Directorate. Member AIAA.

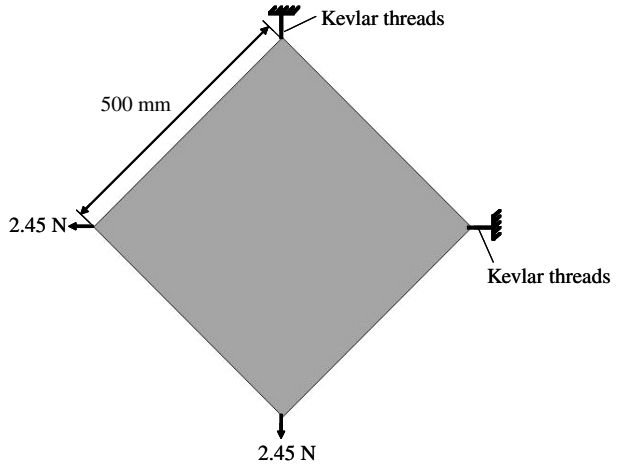


**Fig. 1 Thin-film membrane loaded in tension by corner forces, as tested by Blandino et al. [2].**

## Square Thin-Film Membrane Under Corner Tensile Loads

Recently, Blandino et al. [2] carried out a laboratory test on a 500-mm square flat membrane made of a $2.54 \times 10^{-2}$ mm thick Kapton® Type HN film. The membrane has a $1.0 \times 10^{-3}$ mm thick aluminum coating on one side. The corners were reinforced on both sides with a triangular-shaped 0.12-mm-thick transparency film with dimensions of approximately $10.0 \times 10.0 \times 14.1$ mm. The membrane's overall dimensions and loading are shown in Fig. 1, and the material properties are shown in Table 1. The membrane is subjected to tensile corner loads ($F = 2.45$ N) applied at discrete points via Kevlar® threads that are looped through small pin holes on the left and bottom corners of the membrane. The top and right corners of the membrane are anchored to the test frame with Kevlar threads.

**Table 1 Material properties of 500-mm square thin-film membrane**

| Component | Material | E, N/m$^2$ | $\nu$ |
|---|---|---|---|
| Membrane | Kapton HN | 2.5E + 9 | 0.34 |
| Corner reinforcement | Mylar | 3.8E + 9 | 0.30 |
| Thread | Kevlar | 7.1E + 10 | 0.36 |

In a shell finite element model, in which the loading is represented in the form of a concentrated force and applied at a geometric corner of a tensioned membrane, a wrinkled equilibrium state cannot generally be achieved, even with the inclusion of the out-of-plane imperfections. This unexpected anomaly can be attributed to a severe stress and strain-energy concentration in the region of the applied loading. Because the wrinkling deformations are associated with a very small amount of bending strain energy, the numerical solution, dominated by the markedly high membrane strain energy in a local corner region from which wrinkles emanate, tends to bias the solution toward the membrane state.

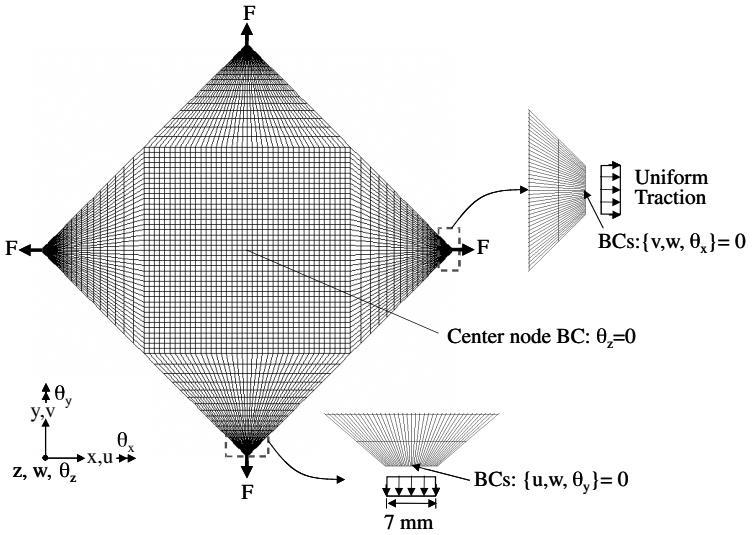


**Fig. 2 Shell finite element model of a thin-film membrane loaded in tension by corner tractions (BC denotes kinematic boundary conditions).**

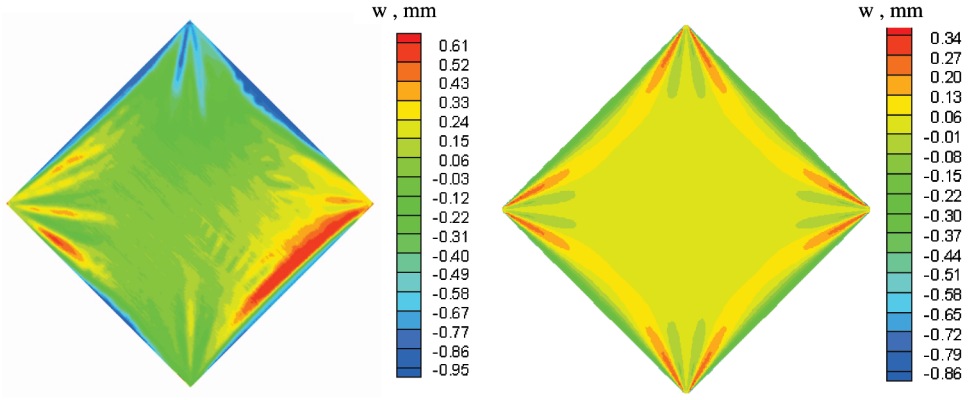


**a) Experiment [2]** **b) ABAQUS FEM results**

**Fig. 3 Wrinkling deformations of a thin-film membrane loaded in tension by symmetric corner loads (BC denotes kinematic boundary conditions).**

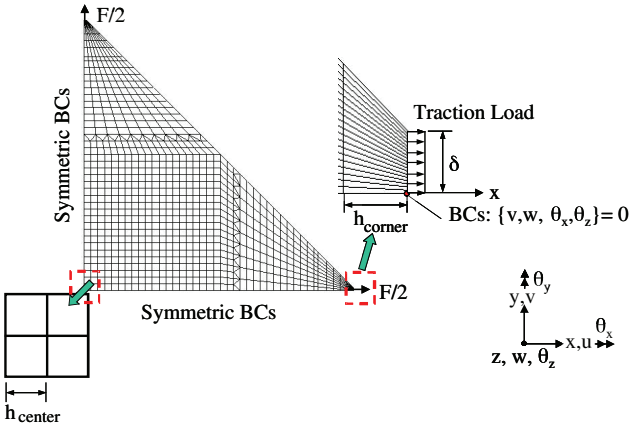


**Fig. 4 Symmetric-quadrant model of a thin-film membrane loaded in tension by corner tractions.**

Recent computational studies [3,4] have shown that structural wrinkles can be produced with the shell finite element models that have no sharp-corner regions and in which concentrated forces are replaced by statically equivalent distributed tractions. Such models lend themselves to improved load transfer and mesh quality, and they mitigate artificially high stress concentrations in the critical corner regions from which wrinkles radiate.

The preceding modeling philosophy was previously demonstrated on the square thin-film membrane subjected to symmetric corner tensile loads [3]. In the finite element model used in the previous study, the corners of the square membrane were truncated, as shown in Fig. 2. The size of the corner truncation was chosen to replicate in a simple, albeit rudimentary, way the reinforcement conditions used in the experiment; thus, a more precise reproduction of the reinforced triangular patches in the corner regions was not attempted. Alternative modeling schemes or loading conditions were not considered in the previous study. The domain of the entire membrane was discretized with a relatively refined mesh of 4720 four-node shell elements in anticipation that such a model could result in a suitable qualitative comparison with the experiment. The finite element mesh was augmented by pseudorandom, out-of-plane imperfections distributed over the interior nodes of the model, with amplitudes of 10% of the membrane thickness, according to

$$z_i = 0.10 p_{ri} h \qquad (i = 1, N) \tag{1}$$

where $p_{ri} \in [-1, 1]$ is a pseudorandom number, $h$ is the membrane thickness, and $N$ is the number of nodes with the imposed imperfections. It was shown that imperfection amplitudes, ranging from 1 to 100% of the membrane thickness, predict practically the same wrinkling deformations, and that the imperfections need only be imposed near the truncated corner regions.

The contour plots depicting the wrinkling-displacement patterns for the square thin-film membrane in the experiment [2] using capacitance sensor measurement and the ABAQUS geometrically nonlinear shell analysis presented in [3] are shown in Fig. 3. The computational model is able to predict four wrinkles radiating from the truncated corner regions, closely correlating with those observed in the experiment. The analysis also predicts that curling occurs at the free edges, as observed in the experiment, although the experiment

**Table 2 Study of element size ratio λ**

| Element size ratio λ | Number of elements | Development of wrinkling deformations |
|---|---|---|
| 0.1 | 1480 | No |
| 0.2 | 1260 | No |
| 0.3 | 1160 | Yes |
| 0.4 | 1080 | Yes |
| 0.5 | 1020 | Yes |
| 0.75 | 940 | Yes |
| 1.0 | 880 | Yes |

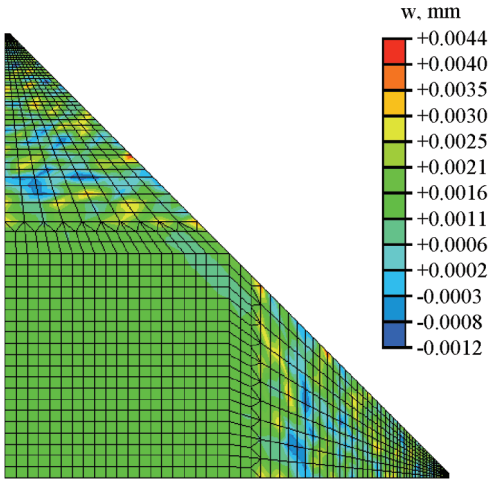


**Fig. 5 Out-of-plane deformations corresponding to the λ = 0.1 symmetric-quadrant model.**

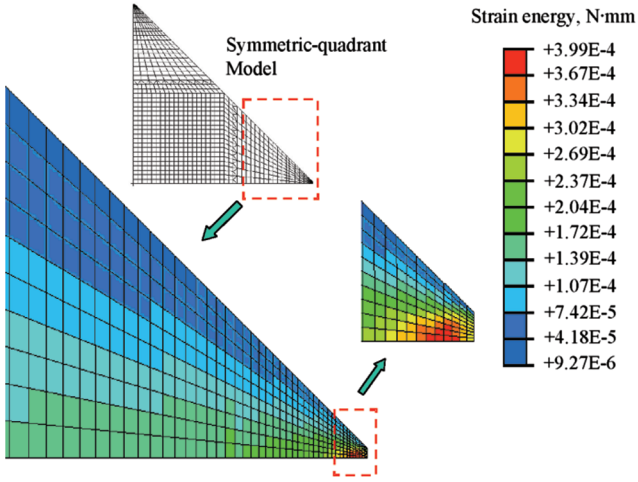


**Fig. 6 Strain-energy contours corresponding to the λ = 0.1 symmetric-quadrant model.**

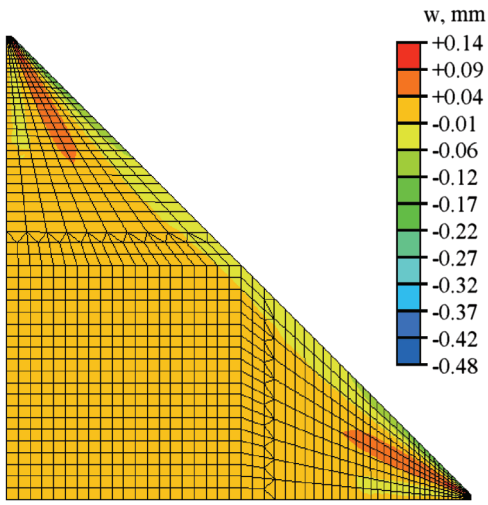


**Fig. 7 Wrinkle-deflection contours corresponding to the λ = 0.3 symmetric-quadrant model.**

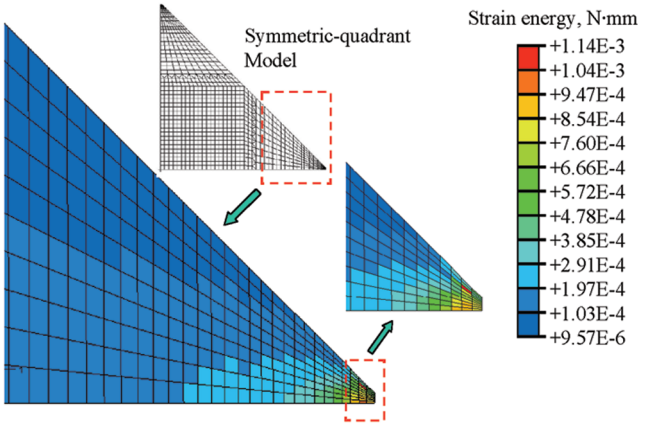


**Fig. 8 Strain-energy contours corresponding to the $\lambda = 0.3$ symmetric-quadrant model.**

shows somewhat greater wrinkle amplitudes. Considering a number of simplifications in the computational model (i.e., not attempting to account for the actual imperfections, corner boundary conditions, gravity effects, and inherent asymmetry of the experimental setup), the comparison with the experiment should only be judged from the qualitative point of view. In this regard, the computational simulation can be viewed as highly successful.

In what follows, two numerical studies are discussed for the square thin-film membrane in tension to ascertain the key factors for modeling wrinkling deformations. The first study addresses the question of how mesh refinement in the region of stress concentration affects the computational model's ability to produce wrinkling deformations. The second study examines how the truncated corner size influences the formation of wrinkles in the computational model. In all cases, uniform tensile tractions are applied along the truncated corner edges, with the total load maintained as a constant. Pseudorandom out-of-plane imperfections are imposed in a symmetric fashion with respect to the four corners of the membrane, with their magnitudes maintained at 10% of the membrane thickness.

In all cases, uniform tensile tractions are applied along the truncated edges at the corners, and small (as compared with the membrane thickness) pseudorandom imperfections are imposed in a symmetric fashion with respect to the four corners of the membrane. A geometrically nonlinear, updated Lagrangian shell formulation [10] is employed to simulate the formation of wrinkled deformations. Use is made of the four-node S4R5 shell element based on large displacements and small strains. The element employs reduced integration of the transverse shear energy and a numerical Kirchhoff correction factor to ensure locking-free behavior in the ultrathin regime of bending. The element formulation also uses an hourglass control method to suppress spurious hourglass modes that result from reduced integration.

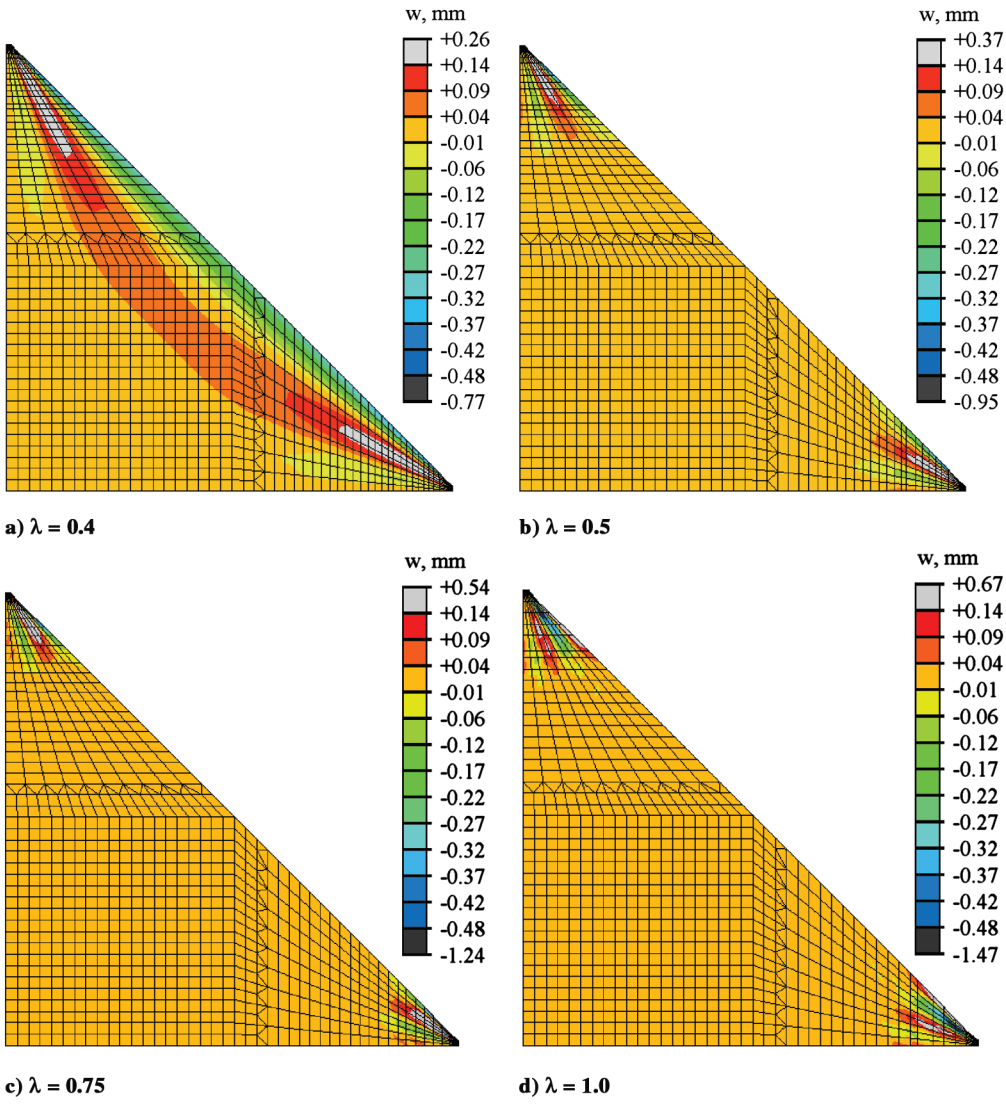


**Fig. 9 Wrinkle-deflection contours for symmetric-quadrant models with various element size ratios.**

### Mesh Refinement at Truncated Corners

The effects of various mesh refinements near the truncated corners of the membrane are investigated to ascertain their influence on the formation of wrinkles. To take advantage of the problem symmetry, a single symmetric quadrant is modeled, as illustrated in Fig. 4. In this model, the truncated corner edge size is set as $\delta = 3.52$ mm.

The study uses an element size ratio defined as $\lambda = h_{\text{corner}}/h_{\text{center}}$, where $h_{\text{corner}}$ and $h_{\text{center}}$ denote, respectively, the typical element dimensions in the truncated corner (near-field) and center model (far-field) regions (refer to Fig. 4). Seven meshes were generated, each corresponding to a different $\lambda$ ratio ($\lambda = 0.1, 0.2, 0.3, 0.4, 0.5, 0.75$, and 1.0), where a larger $\lambda$ indicates a coarser mesh in the truncated corner region.

Table 2 summarizes the information concerning the model data and wrinkling predictions. In contrast to customary expectations, the meshes with the greater number of elements and higher degree of refinement in the stress-concentration regions ($\lambda = 0.1$ and 0.2) produced no wrinkling, that is, the resulting solutions were confined exclusively to membrane deformations. A contour plot of the out-of-plane displacements for the $\lambda = 0.1$ model is shown in Fig. 5. Effectively, only the out-of-plane imperfections, which were initially imposed on the model, are shown as the small out-of-plane disturbances. The distribution of the strain energy, illustrated in Fig. 6, reveals that the free edge of the membrane has very low strain energy, almost two orders of magnitude lower than the energy in the load application region. With a very fine mesh near the load application, the analysis is favoring the membrane stress state, which is manifested by a high strain energy, over the lower strain-energy mode associated with the membrane-to-bending coupling and the ensuing wrinkling mode. Therefore, wrinkling deformations were not able to develop using the superior level of refinement in the region of stress concentration. A closer look at the load application region shows that the maximum strain energy is near the lines of symmetry and away from the free edges of the membrane, the regions that, according to experimental observations, undergo the largest amount of out-of-plane displacement. The $\lambda = 0.2$ model produced similar results for the out-of-plane displacements and strain energy.

Simply by making the mesh coarser in the sharp-corner regions in which the load is applied, the computational models corresponding to the $\lambda = 0.3$, 0.4, 0.5, 0.75, and 1.0 meshes, having overall fewer degrees of freedom, were able to reproduce the highly pronounced wrinkle patterns. The contour plot in Fig. 7, corresponding to the $\lambda = 0.3$ model, shows highly pronounced wrinkles, in which the maximum amplitudes approach 19 times the membrane thickness. The pseudorandom imperfections applied to the initial geometry are two orders of magnitude smaller than the wrinkling displacements and do not provide any measurable contribution to the deformed structural shape. The corresponding strain-energy distribution, shown in Fig. 8, indicates that the maximum strain-energy region has moved closer to the free edge and away from the symmetry line. As shown in Fig. 9, the $\lambda = 0.4$, 0.5, 0.75, and 1.0 meshes were also able to generate deep wrinkles, having similar strain-energy distributions as in the $\lambda = 0.3$ model (not shown). A detailed examination of wrinkling displacements, which also includes the results for the $\lambda = 0.3$ model, is provided in Fig. 10, in which the wrinkled surface is cross-sectioned along two different directions in the close vicinity of the truncated corner region. It is seen that the length of the wrinkles decreases as $\lambda$ increases and that the $\lambda = 0.3$ model generates the longest wrinkles with the lowest amplitudes. In addition, as $\lambda$ increases, the length of the wrinkles decreases and their deflection amplitudes increase.

The wrinkling-deformation patterns corresponding to the various meshes examined thus far were shown to be associated with different strain-energy distributions, especially over the truncated corner regions. Thus, in search for an optimal meshing scheme, a local energy-based criterion appears to emerge. Figure 11 shows a graph of a normalized, maximum element strain-energy density, $U_o = U^e_{o(\max)}/U^e_{o(\max)}$ ($\lambda = 1$), plotted versus the corresponding mesh type designated by $\lambda$. In the preceding expression, $U^e_{o(\max)} = U^e_{(\max)}/A^e$, where $U^e_{(\max)}$ denotes the highest shell-element strain energy across the entire mesh, $A^e$ is the element's reference area, and $U^e_{o(\max)}$ ($\lambda = 1$) denotes the maximum element strain-energy density corresponding to the $\lambda = 1$ mesh. The graph shows that $U_o$ may attain the highest value between $\lambda = 0.4$ and 0.5. Note that these two models produce the largest wrinkling regions, having amplitudes closely resembling those in the experiment (see Fig. 3). This graph also suggests that a $U^e_{o(\max)}$-based criterion could be effective in facilitating automated, adaptive mesh refinements for thin-film membranes undergoing wrinkling deformations.

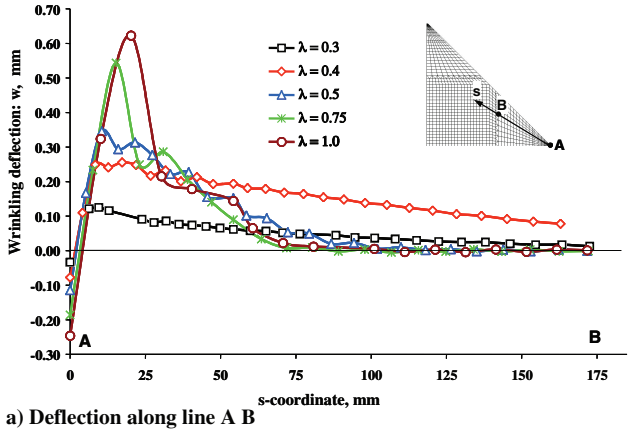


a) Deflection along line A B

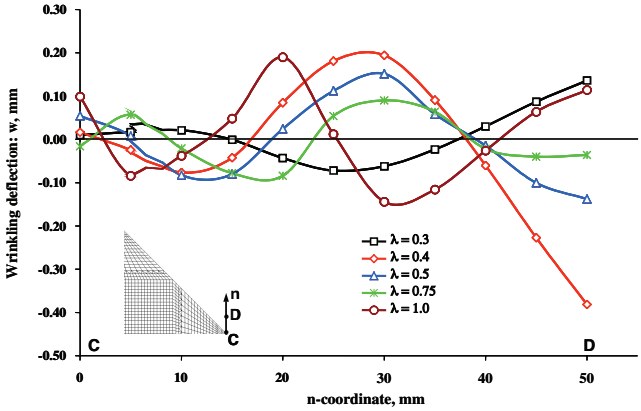


b) Deflection along line C D

**Fig. 10 Comparison of wrinkle deflections as a function of the element size ratio.**

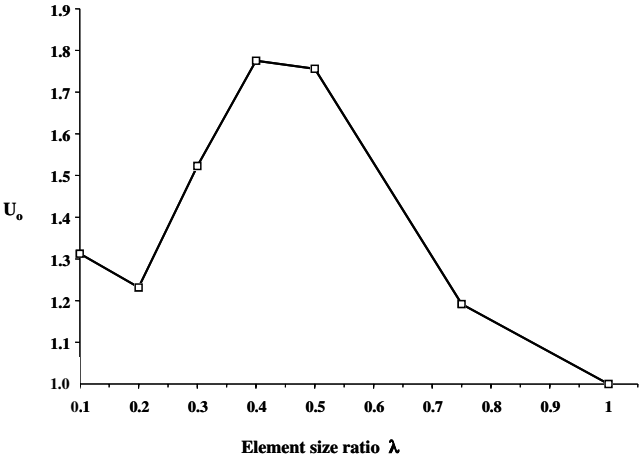


**Fig. 11 Maximum element strain-energy density for the mesh refinement study.**

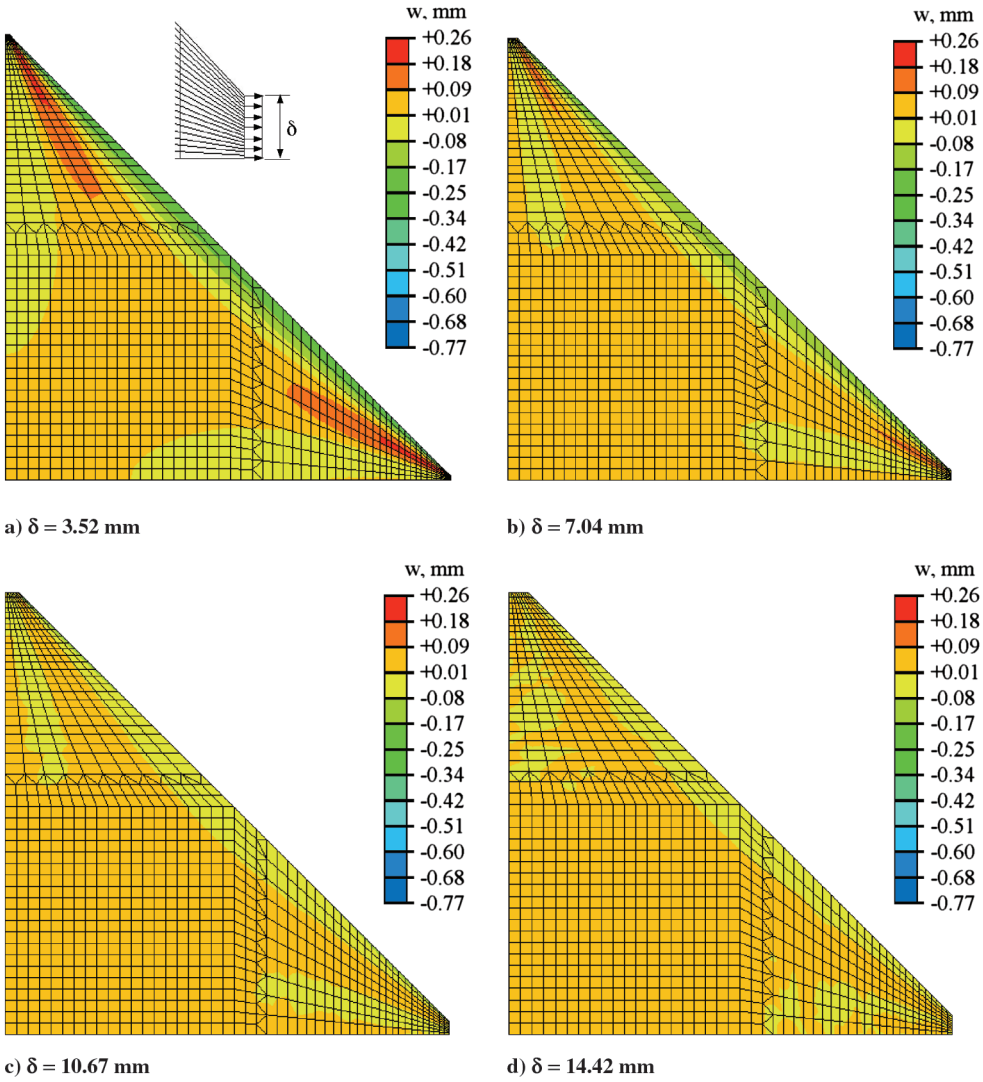


**Fig. 12 Wrinkle-deflection contours corresponding to various truncated corner sizes.**

### Varying Size of Truncated Corners

In this study, the truncated corner size is varied to identify the significance of the load introduction detail and its influence on the prediction of wrinkles. Here, four different models were examined, each corresponding to the truncation size of $\delta = 3.52$, 7.04, 10.67, and 14.42 mm, using the $\lambda = 0.4$ mesh that was perceived as *optimal* from the first study. The various $\delta$-truncation models were achieved by removing elements along the truncated edge in the finite element model. As implemented in the first study, symmetric out-of-plane imperfections were imposed in the corner regions of the membrane, with their magnitudes set at 10% of the membrane thickness. Moreover, statically equivalent distributed tractions were imposed along the corner truncation edges.

The wrinkling-displacement contours corresponding to the four $\delta$-truncation models are shown in Fig. 12. The results show that the length of the wrinkles decreases as the edge length of the truncated corner $\delta$ is increased. Moreover, the wrinkle amplitudes tend to decrease as $\delta$ is increased. The last case, for $\delta = 14.42$ mm, shows a dramatically deteriorating wrinkle pattern, indicating that the solution is biased toward the membrane state. A closer look at the details of the wrinkles is provided in Fig. 13, in which the wrinkled surface is cross-sectioned along two different directions in the close vicinity of the truncated corner region. The results show that the original model with the shortest truncated edge ($\delta = 3.52$ mm) produces the longest and deepest wrinkles. The experimental results in [2] show that the wrinkle amplitude is approximately 0.20 mm. It is also noted that the strain-energy contours (not shown) indicate that strain-energy concentration shifts from being evenly distributed over the truncated corner region for the shortest truncated corner edge to being concentrated along the symmetry line as the truncated corner edge is increased.

## Conclusions

In this paper, two numerical studies were carried out on statically loaded, tensioned, thin-film membranes that have regions of stress concentration and that undergo large out-of-plane wrinkling deformations. The numerical studies focused exclusively on the problem of an initially flat, square thin-film membrane (a solar-sail-like structure) subjected to tensile, in-plane corner loads. The problem, which has attracted considerable attention in recent years, was tested in a structures laboratory and analyzed by various finite element codes to investigate the onset of wrinkling.

In these studies, the effects of mesh refinement and geometry augmentation of the corner (stress-concentration) regions were examined. The analyses used a four-node Mindlin-type quadrilateral shell element, S4R5, based on small strains, large displacements, reduced integration of the transverse shear energy, and an updated Lagrangian frame of reference, as implemented in the ABAQUS finite element code. The key modeling features included specifying small pseudorandom geometric imperfections that enable the initiation of the membrane-to-bending coupling that is necessary to start the onset of wrinkling. The membrane corners were truncated

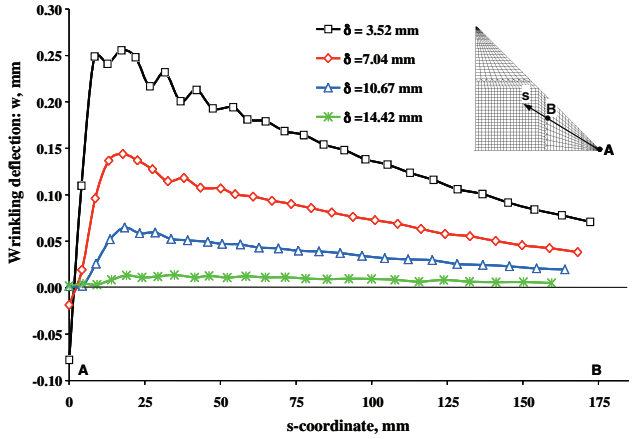


a) Line A B

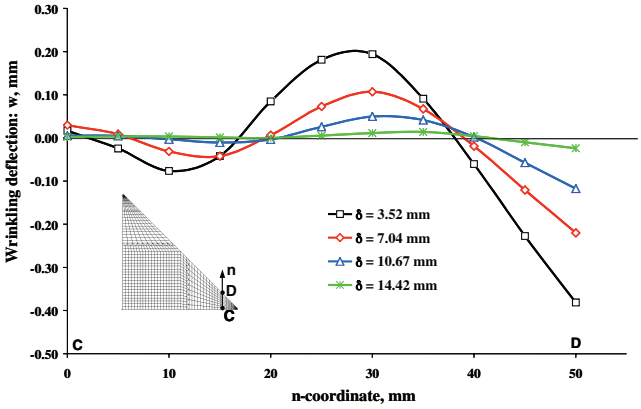


b) Line C D

**Fig. 13 Comparison of wrinkle deflections as a function of a truncated corner size.**

and uniform tensile tractions were applied along the truncated corner edges to reduce the adverse effects of the severe stress concentration.

The first study that concerned itself with the mesh refinement in the corner regions (of high stress concentration) revealed, at first glance, a somewhat counterintuitive result: further refinements of the corner regions generated an entirely membrane response, producing none of the experimentally observed wrinkling deformations. Such a result is clearly due to the basic characteristic of the finite element method that focuses its power primarily on enhancing those modes of deformation that are associated with the higher strain-energy modes. In the present case, however, it is the membrane strain energy that is dominant, especially in the membrane-dominated stress-concentration region. Thus, what is commonly perceived as improved refinement of the stress-concentration regions is actually detrimental for this class of problems in which both low- and high-energy modes of deformation need to be captured; the refinement further suppresses the low-energy modes associated with bending (wrinkling) and effectively biases the solution into the membrane-deformation mode. The study further showed that derefinement of the corner regions is actually beneficial, giving rise to an improved balance in the approximation of the membrane and bending deformations, resulting in wrinkling patterns that compare reasonably well with the experimental observation.

The second study examined the effect of various sizes of the truncated corners on the wrinkling response of a thin square membrane in which the basic mesh characteristics were unchanged. This study was specifically aimed at addressing the question of the sensitivity of the wrinkling response to small geometric changes of the corner (boundary) conditions. It was demonstrated that relatively small changes in the size of the truncated region produced distinctly different wrinkling deformations, including their patterns, wavelength, and depth. This aspect brings the importance of precise modeling of such regions into focus, particularly when specific membrane structures need to be modeled with a high degree of accuracy.

## References

[1] Jenkins, C. H. M. (ed.), "Membrane Wrinkling," *Recent Advances in Gossamer Spacecraft*, Vol. 22, Progress in Astronautics and Aeronautics, AIAA, Reston, VA, 2006, pp. 109–163.

[2] Blandino, J. R., Johnston, J. D., and Dharamsi, U. K., "Corner Wrinkling of a Square Membrane due to Symmetric Mechanical Loads," *Journal of Spacecraft and Rockets*, Vol. 35, No. 9, Sept.–Oct. 2002, pp. 717–724.

[3] Tessler, A., Sleight, D. W., and Wang, J. T., "Effective Modeling and Nonlinear Shell Analysis of Thin Membranes Exhibiting Structural Wrinkling," *Journal of Spacecraft and Rockets*, Vol. 42, No. 2, Mar.–Apr. 2005, pp. 287–298.

[4] Wong, Y. W., and Pellegrino, S., "Computation of Wrinkle Amplitudes in Thin Membrane," 43rd AIAA/ASME/ASCE/AHS/ASC Structures, Structural Dynamics, and Materials Conference, Denver, CO, AIAA Paper 2002-1369, 2002.

[5] Wong, Y. W., Pellegrino, S., and Park, K. C., "Prediction of Wrinkle Amplitudes in Square Solar Sails," 44th AIAA/ASME/ASCE/AHS/ASC Structures, Structural Dynamics, and Materials Conference, Norfolk, VA, AIAA Paper 2003-1982, 2003.

[6] Lee, K., and Lee, S. W., "Analysis of Gossamer Space Structures Using Assumed Strain Formulation Solid Shell Elements," 43rd AIAA/ASME/ASCE/AHS/ASC Structures, Structures Dynamics, and Material Conference, Denver, CO, AIAA Paper 2002-1559, April 2002.

[7] Leifer, J., Black, J. T., Belvin, W. K., and Behun, V., "Evaluation of Shear Compliant Boarders for Wrinkle Reduction in Thin Film Membrane Structures," 44th AIAA/ASME/ASCE/AHS/ASC Structures, Structural Dynamics and Materials Conference, Norfolk, VA, AIAA Paper 2003-1984, Apr. 2003.

[8] Su, X., Abdi, F., and Blandino, J. R., "Wrinkling Analysis of a Kapton Square Membrane Under Tensile Loading," 44th AIAA/ASME/ASCE/AHS/ASC Structures, Structural Dynamics, and Materials Conference, Norfolk, VA, AIAA Paper 2003-1985, 2003.

[9] Wagner, H., "Flat Sheet Girder with Very Thin Metal Web," *Zeitschrift für Flugtechnik und Motorluftschiffahrt*, Vol. 20, pp. 200–207, 227–231, 281–284, 306–314, 1929.

[10] ABAQUS, Software Package, Ver. 6.3.1, Hibbitt, Karlsson, and Sorensen, Inc., Pawtucket, RI, 2002.

M. Nemeth
*Associate Editor*